

LETTER OF INTENTStudy of $\bar{p}p$ and $\bar{p}d$ interactions at threshold
in gaseous H_2 and D_2 targets at LEAR

CERN-LAL-Mainz-München-TRIUMF-Zürich Collaboration *)

R. Armenteros¹, E.G. Auld², D.A. Axen², G.A. Beer³, J.C. Bizot⁴,
M. Comyn⁵, M.K. Craddock², W. Dahme⁶, B. Delcourt⁴, K.L. Erdmann⁵,
P. Eschtruth⁴, U. Gastaldi⁷, G. Gräff⁷, P. Heusse⁴, J. Jeanjean⁴, H. Kalinowsky⁷,
F. Kayser⁷, E. Klempt⁷, R. Landua⁷, C.J. Martoff⁸, Ch. Sabev⁹,
R. Schneider⁷, R. Schulze⁷, U. Sraumann⁸, P. Trüol⁸, J.B. Warren²,
B.L. White², R.W. Wodrich⁷

- 1) CERN, Geneva, Switzerland
- 2) University of British Columbia, Vancouver, Canada
- 3) University of Victoria, Canada
- 4) LAL, Orsay, France
- 5) TRIUMF, Vancouver, Canada
- 6) University of München, W. Germany
- 7) University of Mainz, W. Germany
- 8) University of Zürich, Switzerland
- 9) CERN visitor, Geneva, Switzerland

*) Spokesman: E. Klempt
Contactman: U. Gastaldi

I. PHYSICS

Antiproton nucleon strong interaction at threshold (annihilation, elastic scattering, off shell charge exchange ...) occur in atomic orbitals of the antiprotonic atom that forms when an antiproton is stopped inside a target. Direct evidence of formation of antiprotonic hydrogen and deuterium atoms has been established by detecting the characteristic radiative transitions to the 2P atomic energy level in a recent experiment where, for the first time, use was made of a gas target at room temperature^{1,2}).

At threshold the strong $\bar{N}N$ interaction manifests itself by shifting and broadening the Coulomb levels of $\bar{p}p$ and $\bar{p}d$ atoms³⁻¹⁶), by causing annihilation and by determining the annihilation pattern (branching ratios of annihilation final states for each initial atomic state depopulated by annihilation). Shift ΔE and broadening Γ of the $\bar{p}p$ and $\bar{p}d$ Coulomb atomic levels are expected to depend strongly on the total spin state (hyperfine splitting due to the spin dependence of $\bar{N}N$ forces) and on the existence in the proximity of the threshold of resonances and quasinuclear $\bar{p}N$ bound states in the same spin state. Baryonium states below threshold can be most intensely populated by radiative¹⁰) and pionic¹⁷) transitions from initial atomic states. The strength and the yield of these transitions depend on the strong interaction distortion of the atomic wave functions and on the distribution of initial atomic states.

Antiproton interaction at rest are then of interest for atomic physics (strong interaction shift and broadening of $\bar{p}p$ and $\bar{p}d$ atomic levels, $\bar{p}p$ and $\bar{p}d$ atomic cascades in matter), for nuclear physics (NN and $\bar{N}N$ potentials comparison, quasinuclear bound states of N and \bar{N}) and for particle physics (antiproton as low energy hadronic probe of the inside of the nucleon: annihilation; exotic quark aggregates: baryonium). The atomic, nuclear and particle physics aspects are strictly connected because the phenomenological picture of $\bar{N}N$ strong interactions at rest (annihilation branching ratios, transitions to baryonium) depend on the (n, l) distribution of initial atomic states. This distribution depends on the mixing of atomic levels during collisions and on the annihilation width of S and P atomic levels (Stark mixing¹⁸)). Moreover the Stark mixing depends on the target density and on the strong shift of the S levels.

Investigations of the antiproton-nucleon strong interaction at threshold started with bubble chamber experiments and continued with counter experiments making use of liquid H₂ (D₂) targets. In bubble chamber experiments^{19,27)} branching ratios for annihilation at rest in liquid into pionic and kaonic final states were measured, $\bar{p}N$ coupling to mesonic resonances was studied, evidence of dominant annihilation from initial atomic S-wave orbitals was produced and evidence for $\bar{p}n$ quasinuclear/baryonium bound states was reported. Counter experiments concentrated on rare annihilation channels (e.g. $\bar{p}p \rightarrow e^+e^-$ ²⁸⁾) and on annihilation channels with many neutrals (e.g. $\bar{p}p \rightarrow \pi^0\pi^0$ ^{29,30)}, $\bar{p}p \rightarrow \gamma + \text{anything}$ ^{31,32)}) in the final state. Comparison of $\bar{p}p$ annihilation branching ratios into $\pi^0\pi^0$ and into $\pi^+\pi^-$ pointed to an important P-wave annihilation component in the $\bar{p}p \rightarrow 2\pi$ channel and has cast doubt on the usual assumption of dominant S-wave annihilation in liquid hydrogen supported by bubble chamber data³³⁾. Evidence has been reported of detection of direct γ transitions from initial $\bar{p}p$ atomic states to states below threshold (quasinuclear bound states or baryonium states³⁴⁾). Upper limits for the population of the $\bar{p}p$ atom ground state 1S are available. These limits depend strongly on the assumption made on the width of the K lines and range from some 10^{-4} in liquid H₂^{35,36)} to 10^{-2} in H₂ and D₂ gas at 4 atm^{1,2)}. Atomic P-wave annihilation has been observed directly in the 2P level of $\bar{p}p$ and $\bar{p}d$ atoms^{1,2)}, but only a lower limit $\Gamma_{\text{ANN}} \geq 10\Gamma_{\text{RAD}}$ for the 2P level annihilation width is available.

The existing picture of $N\bar{N}$ interactions at rest is clearly far from being complete:

- i) there is no direct measurement of the $\bar{p}p$ and $\bar{p}d$ S-wave scattering length and of the P-wave scattering volume;
- ii) the (density dependent) balance between S-wave and P-wave annihilation is not known (existing branching ratios of annihilation channels are inclusive on all the initial atomic states compatible with the selection rules);
- iii) evidence for baryonium below threshold is weak and quantum numbers cannot be attributed to present candidates.

The main limits of present day experimental approaches are due to the use of liquid targets:

- a) the rate of γ/π transitions to high angular momentum baryonium states near threshold is damped by the intense Stark mixing that depresses the population of the low n atomic states;
- b) the quantum numbers of the initial atomic states from which annihilation and transitions to baryonium may occur cannot be measured directly because of the scarcity of detectable X-rays and the incompatibility of a large acceptance detector for low energy X-rays with a liquid target.

Notwithstanding the points indicated above, all experiments presently on the floor at CERN and Brookhaven to search for baryonium transitions from protonium make use of liquid targets. This is somewhat imposed by the nature of present low energy antiproton beams in order to get a significant amount of \bar{p} stops in the experimental target.

At LEAR the low momentum and momentum dispersion of the extracted antiproton beam will permit to stop abundantly antiprotons also in a gas target, that can be combined with an X-ray detector of low energy threshold.

We intend therefore to perform at LEAR a study of $\bar{p}p$ and $\bar{p}d$ interactions at threshold by stopping antiprotons in a gaseous target and by using a detection system with large angular acceptance designed to

- 1) detect the K, L and M X-rays of $\bar{p}p$ ($\bar{p}d$) atomic transitions ($\sim 10, 2$ and 1 KeV respectively);
- 2) measure with a magnetic spectrometer the momentum of \bar{p} annihilation prongs;
- 3) detect with good spacial localization gammas associated to \bar{p} annihilations.

The experimental set up that we envisage combines the new features of a gas target and an efficient X-ray detector intended primarily for triggering and flagging purposes³⁷). The completeness and sophistication of the detection capability of our apparatus for annihilation products would be balanced with the aim of starting experimentation as soon as LEAR is ready.

Our physics goals concern three main sectors:

- a) Protonium spectroscopy
- b) $\bar{p}p$ annihilation
- c) Baryonium (via protonium), and the corresponding $\bar{p}d$ cases (the extension to $\bar{p}d$ is assumed and will no more be explicitly mentioned from now onwards).

Also use of the experimental set up for later measurements in flight at low kinetic energies is considered.

a) Protonium spectroscopy

By detecting radiative transitions to the $n = 1$ levels of $\bar{p}p$ and $\bar{p}d$ atoms (K-lines) we could obtain the spin dependent $\bar{p}p$ ($\bar{p}d$) complex S-wave scattering length a from the measurement of shift and width of the levels:

$$\Delta E + i \frac{\Gamma}{2} = \frac{-1}{2m} |\psi_{1S}(0)|^2 a.$$

We will try to resolve the ground state hyperfine structure and to measure ΔE and Γ of each hyperfine sublevel, by selecting K X-rays in coincidence with specific annihilation channels allowed only from one given initial spin state (e.g. $\bar{p}p$ K X-rays detected in coincidence with annihilation into neutral pions only must have populated the singlet 1^1S_0 state).

The $\bar{N}N$ scattering length in a given spin and isospin channel is expected to be influenced by the existence of quasinuclear or baryonium states near threshold in the same channel. Determination and comparison of scattering lengths in the $\bar{p}p$ and $\bar{p}d$ channels may therefore help to assign quantum numbers to baryonium states established in independent experiments or point to their existence.

We intend to measure the annihilation width Γ_{2P} of the 2P level by comparing the intensity of the K_α X-ray line (2P-1S transitions) to the intensity of the L lines that populate the 2P level. The yield of L X-rays in gas at 4 atm NT is $\sim 5\%^{1,2}$). We expect a higher yield at 1 atm NT. The lower limit on Γ_{2P} was obtained at 4 atm by counting the number of X-rays in the K line energy region that were in coincidence with a L X-ray. This coincidence technique is extremely powerful in reducing background. Our X-ray detector will optimize the detection efficiency and maximize the background rejection for X-rays in the L energy region to allow systematic use of the L X-ray coincidence technique. Extension of the technique to clean the L X-ray spectrum can be envisaged by requiring a M X-ray in coincidence.

Measurements of the yield of K, L and M lines independently and in coincidence will give information on the development of the atomic cascade.

b) $\bar{p}p$ annihilation

We intend to measure annihilation branching ratios focussing attention on the two body annihilation channels $\pi^+\pi^-$, K^+K^- , $K_S^0 K_L^0$, $K_S^0 K_S^0$ that can be identified unambiguously by the magnetic spectrometer. Also the inclusive branching ratios with 2, 4, 6 charged particles and any number of neutrals could be measured.

By exploiting the X-ray information it will be possible to measure and compare:

- i) inclusive branching ratios (no X-ray trigger);
- ii) b.r. for annihilations in the 2P level (L X-ray in coincidence);
- iii) b.r. for annihilations in the 1S level (K X-ray in coincidence).

If the hyperfine splitting of the 1S levels turn out to be appreciable it will then also be conceivable to compare S-wave annihilation reactions from states of different spin.

c) Baryonium

We intend to search for baryonium states reached from protonium levels with a radiative or pionic transition by analyzing events with at most one neutral in the final state. By discarding those events where some prongs escaped the spectrometer chambers these reactions will be kinematically constrained because, due to the little scattering in the gas target and the surrounding X-ray detector, it will be possible to reconstruct precisely both the missing mass and the missing momentum.

We consider in particular the following set of possible transitions:

$$\begin{aligned} \bar{p}p &\rightarrow B + \gamma & (1) \\ &\downarrow \\ &\pi^+\pi^- \\ &2\pi^+2\pi^- \\ &K^+K^- \end{aligned}$$

$$\begin{aligned} \bar{p}p &\rightarrow B + \pi^0 & (2) \\ &\downarrow \\ &\pi^+\pi^- \\ &2\pi^+2\pi^- \\ &K^+K^- \end{aligned}$$

$$\begin{aligned} \bar{p}p &\rightarrow B + \pi^\mp & (3) \\ &\downarrow \\ &2\pi^\pm\pi^\mp \\ &\pi^\pm\pi^0 \\ &2\pi^\pm\pi^\mp\pi^0 \end{aligned}$$

for which a baryonium level narrower than the experimental resolution produced with a 10^{-3} branching ratio would give a better than 5 to 10 standard deviation peak to background signal for 10^9 triggers. Reaction (1) would be particularly clean because the direction of the missing momentum would also be defined by the annihilation vertex and the γ conversion point and no direct coincident background is expected. Both negative and positive G parity baryonium states are accessible by one or the other of these reactions.

To increase the probability of reaching a narrow baryonium state of high angular momentum we would trigger on events with a detected L X-ray. Comparison with spectra without the L X-ray trigger would allow us to restrict or fix the quantum numbers of peaks appearing in the data.

Experiments in flight

A natural extension of our programme which is envisageable with no major modifications to the experimental apparatus would be to study the low energy region above threshold that is at present unexplored.

We would then envisage a search for the formation of narrow baryonium resonances and study the energy dependence of σ_{TOT} , $\sigma_{\pi^+\pi^-}$, $\sigma_{K^+K^-}$, $\sigma_{K_S^0 K_S^0}$, σ_{ANNIH} and σ_{e1} . The two body annihilation channel could be studied with good resolution because of the constrained kinematics.

II EXPERIMENTAL SET-UP

Apparatus

A sectional view of the general layout of the experimental apparatus cut along a horizontal plane containing the beam axis is shown in Fig. 1.

The central part of the set-up is a system that includes

- i) a cylindrical gas H_2 target;
- ii) a surrounding X-ray detector (XDC for X-ray drift chamber);
- iii) a multicell cylindrical drift chamber (IDC) envelopping the XDC.

The H_2 gas where antiprotons are brought to rest is contained in a very thin aluminized mylar tube that has good transmission for the low energy $\bar{p}p$ X-rays and is installed and kept in cylindrical shape following a

well tested technique³⁸). The XDC is a cylindrical drift and proportional multiwire chamber with radial drift direction capable of detecting and identifying low energy X-rays down to 500 eV^{39,40}). The IDC works with the same gas mixture of the XDC, supplements the XDC for detecting $\bar{p}p$ K line X-rays and detects with good accuracy in $\emptyset \bar{p}$ annihilation prongs from the H₂ target.

The assembly H₂ target/XDC/IDC is installed in the centre of a magnetic spectrometer consisting of four extra light cylindrical MWPC's (each with read out from the anode and the cathodes) located inside a 1.2 m long \emptyset 1.7 m solenoid with 0.8 T top field. We plan to use the solenoid and the chambers of the DMI spectrometer^{41,42}) which has terminated its operations at the DCI e⁺e⁻ storage ring at LAL, Orsay (Fig.2).

Position sensitive γ detectors (lead plates and MWPC sandwiches) are installed at the end caps of the solenoid to count γ 's, measure the conversion point of γ 's from neutral transitions to baryonium and possibly determine the energy of monochromatic π^0 transitions from a measurement of the opening angle of the two photon π^0 decay⁴³).

Position sensitive γ detectors are also located between the coil and the return iron yoke.

The characteristics of the main components of the apparatus are summarized in Table 1.

By concentrating our hardware effort on the detectors for neutrals (X and γ) we should be able to get, combining with DMI, a fairly good detection system tested and ready to take data at the start of LEAR operation.

Our set up will also be suitable to study with high resolution $N\bar{N}$ interactions in flight at low energy by equipping the gas target with extremely thin entrance and exit windows, by letting the \bar{p} beam traverse it and by recording the interactions in a fiducial volume inside the gas. The XDC could be used in this case to also detect low energy recoil protons.

An extension of the position sensitive γ detection to a 4π coverage inside the coil could be envisaged in a successive step that would exploit the solenoid, the XDC assembly and the end cap γ detectors.

Beam

In order to stop the maximum amount of antiprotons in the centre of the gas target we will reduce the energy of the beam extracted from LEAR with a moderator installed inside the magnetic volume at the entrance of the gas target. Our target (~ 80 cm long, H_2 gas NTP will be ~ 7 mg cm^{-2} thick. With the 300 MeV/c $\Delta p/p < 10^{-3}$ \bar{p} beam expected in the first phase of LEAR operation we will have a rather flat distribution of \bar{p} stops along the axis of the detector and $\sim 2/3$ of the antiprotons will annihilate in the moderator and in a downstream veto counter. With a 100 MeV/c $\Delta p/p < 10^{-3}$ \bar{p} extracted beam obtainable by implementing electron cooling in LEAR, the situation would improve substantially as the \bar{p} stop distribution would concentrate at the centre of the target in a volume shorter than 10 cm. This would imply easier pattern recognition and a higher angular acceptance of the detection system.

The rate of firing of the detectors will be fairly independent of the beam momentum for $P_{\text{beam}} < 300$ MeV/c, as in all cases annihilation will occur dominantly at rest and inside the magnetic volume of the spectrometer. The maximum beam intensity that can be used in stop experiments is limited to $\sim 10^5$ sec^{-1} due to the long drift time in the XDC cells. During first survey measurements with loose trigger conditions we will need a beam of lower intensity due to saturation of the data acquisition system. During later experiments in flight we could have the whole LEAR beam ($\sim 10^6$ \bar{p} sec^{-1}) traversing the H_2 target.

III. PRIORITIES AND INDICATIONS

Our priority regarding the additional options considered for LEAR goes naturally to electron cooling that would allow us to get a better stop distribution due to the lower beam momentum and momentum dispersion obtainable.

The research programme that we would like to pursue is an extrapolation to LEAR conditions of research work started years ago by part of the present collaboration at the CERN PS^{1,2}). Testing and design work in the perspective indicated in this letter is currently under way in some of the collaborating institutes. However funding is bound for some institutes to having an approved proposal. Since time may become limited to get the whole set up

ready for the start up of LEAR it would therefore be convenient for us to have an early call for proposals, so as to have the possibility of getting a decision concerning our proposal by the middle of 1980.

TABLE 1
Characteristics of the detection system

Particle	Detector	Solid angle $\Omega/4\pi$ (%)	Detection efficiency η (%)	$\frac{\Omega\eta}{4\pi}$ (%)	Spatial resolution (σ)	Resolution (FWHM) ↓	Note	Ref.
X-ray	XDC	>90	>20	20	$\Delta R \otimes \Delta \phi \otimes \Delta Z$ $0.5 \times 2 \times 10 \text{ mm}^3$	$\Delta E/E \sim$ $20\% \sqrt{\frac{E}{5.5 \text{ keV}}}$ + XDC discrim.	a	38, 39
Prongs	Spectrometer	60	99	60	$R \Delta \phi \times \Delta Z$ $0.6 \times 1.7 \text{ mm}^2$	$\Delta p/p \sim$ $6\% \frac{p(\text{MeV})}{500}$		41, 42
	XDC	>90	99	>90	$R \Delta \phi \times \Delta Z$ $2 \times 10 \text{ mm}^2$			
	IDC	>90	>95	>90	$R \Delta \phi \times \Delta Z$ $0.2 \times 10 \text{ mm}^2$			
γ	PSGD	50	>90	>45	$2 \times 2 \text{ mm}^2$		b	
	GD	40	50	20			b	
π^0	PSGD			20		$\Delta E/E \sim$ $1\% \frac{E(\text{MeV}) - 50}{140}$	b, c	43

a) Detection threshold $\sim 300 \text{ eV}$

Efficiency $\eta > 20\%$ with 6μ mylar tube and Ar counter gas for X-rays with energy $E > 1.5 \text{ KeV}$.

b) Efficiencies are computed for 100 MeV gammas.

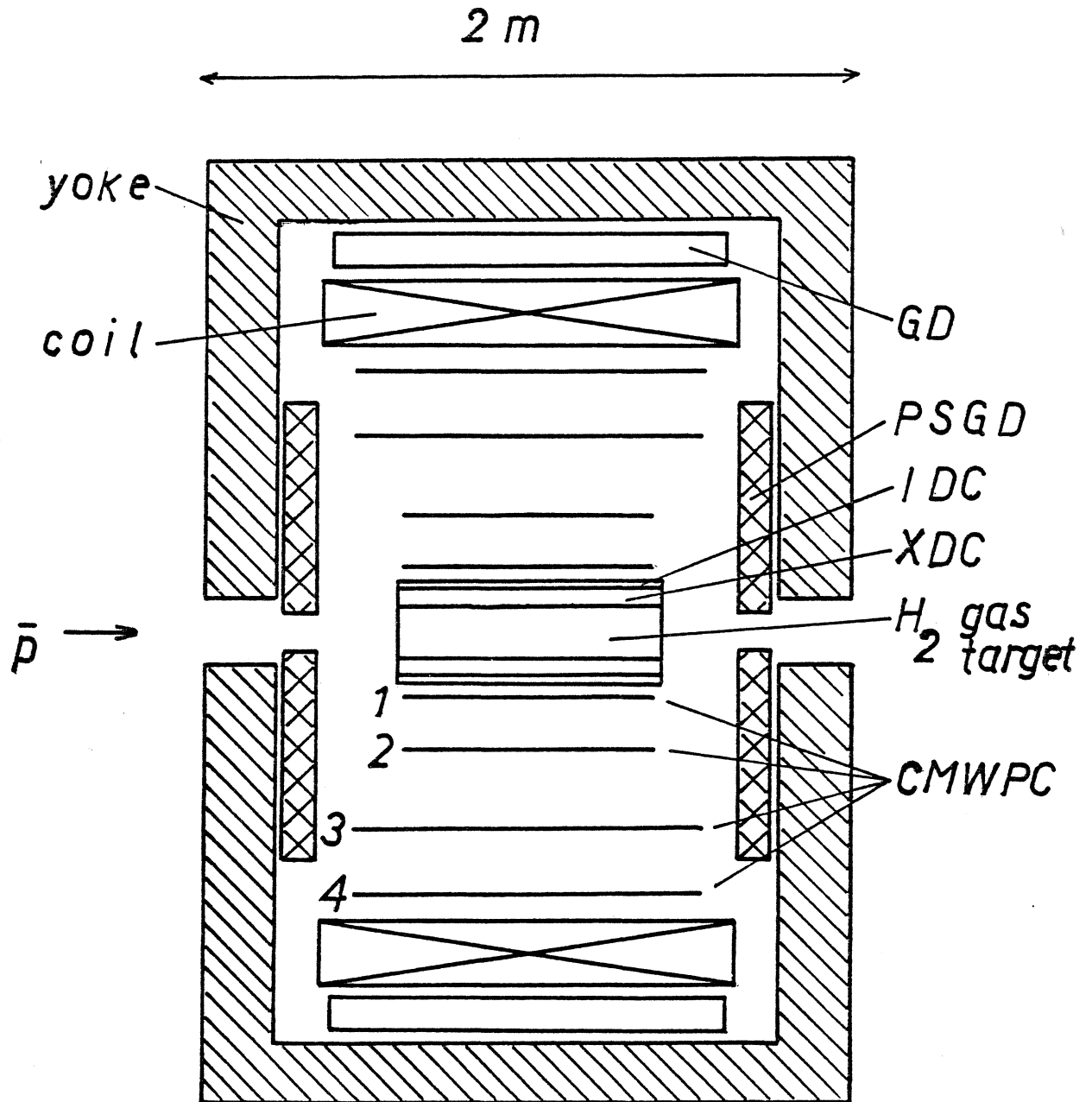
c) 17 mrad resolution on the opening angle of the two γ 's from a single π^0 with 1 mm^3 granularity in the \bar{p} annihilation vertex reconstruction.

REFERENCES

- 1) E. Auld et al., Phys. Lett. 77B (1978) 454.
- 2) E. Auld et al., *in* Proc. 4th European Antiproton Symposium, Barr-Strasbourg, 1978 (ed. A. Friedman) (Editions du CNRS, Paris, 1979), Vol. 1, p. 115.
- 3) S. Caser and R. Omnès, Phys. Letters 39B (1972) 369.
- 4) O.D. Dalkarov and V.M. Samoïlov, JETP Letters 16 (1972) 249.
- 5) O.D. Dalkarov and B.O. Kerbikov, JETP Letters 21 (1975) 134.
- 6) V.E. Markushin, Preprint ITEP-164, Moscow (1976),
- 7) W.B. Kaufmann and H. Pilkuhn, Phys. Letters 62B (1976) 165.
- 8) T.E.O. Ericson, Low-energy $\bar{N}N$ interactions, Proc. 3rd European Symposium on Antinucleon-Nucleon Interactions, Stockholm, 1976 (eds. G. Ekspong and S. Nilsson) (Pergamon Press, Oxford, 1977), p. 3.
- 9) T.E.O. Ericson and L. Hambro, Ann. Phys. 107 (1977) 44.
- 10) O.D. Dalkarov, Preprint ITEP-135, Moscow (1977).
- 11) B. Kerbikov, Preprint CERN-TH 2394 (1977).
- 12) I.S. Shapiro, Phys. Reports 35C (1978) 131.
- 13) A.E. Kudryavtsev, V.E. Markushin and I.S. Shapiro, Sov. Phys. JETP 47 (1978) 225.
- 14) W.B. Kaufmann and H. Pilkuhn, Phys. Rev. C 17 (1978) 215.
- 15) W.B. Kaufmann, Phys. Rev. C 19 (1979) 440.
- 16) W.B. Kaufmann, Contributed paper to ICOHEPANS 8th, Vancouver, 1979.
- 17) C.B. Dover and M.C. Zabek, Phys. Rev. Lett. 41 (1978) 438.
- 18) T.B. Day, G.A. Snow and J. Sucher, Phys. Rev. 118 (1960) 864.
- 19) For a review of work previous to 1969, see R. Armenteros and B. French, $\bar{N}N$ interactions, *in* High energy physics (ed. E.H.S. Burhop) (Academic Press Inc., New York, 1969), Vol. 4, p. 383.
- 20) L. Gray et al., Phys. Rev. Letters 26 (1971) 1491.
- 21) P. Frenkiel et al., Nuclear Phys. B47 (1972) 61 and references quoted therein.

- 22) L. Gray et al., Phys. Rev. Letters 30 (1973) 1091.
- 23) R. Bizzarri et al., Nuclear Phys. B69 (1974) 298.
- 24) R. Bizzarri et al., Nuclear Phys. B69 (1974) 307.
- 25) T.E. Kalogeropoulos and G.S. Tsanakos, Phys. Rev. Letters 34 (1975) 1047.
- 26) T.E. Kalogeropoulos and G.S. Tsanakos, *in* Proc. 3rd European Symposium on Antinucleon-Nucleon Interactions, Stockholm, 1976 (eds. G. Ekspong and S. Nilsson) (Pergamon Press, Oxford, 1977), p. 29.
- 27) C.R. Sun et al., Phys. Rev. D 14 (1976) 1188.
- 28) G. Bassompierre et al., Phys. Letters 64B (1976) 475.
- 29) S. Devons et al., Phys. Rev. Letters 27 (1971) 1614.
- 30) G. Bassompierre et al., *in* Proc. 4th European Antiproton Symposium, Barr-Strasbourg, 1978 (ed. A. Friedman) (Editions du CNRS, Paris, 1979), Vol. 1, p. 139.
- 31) T.E. Kalogeropoulos et al., Phys. Rev. Letters 35 (1975) 824.
- 32) P. Pavlopoulos et al., Phys. Letters 72B (1978) 415.
- 33) For a review, see R. Bizzarri, *in* Proc. Symposium on Antinucleon-Nucleon Annihilations, Chexbres, 1972 (ed. L. Montanet) (CERN 72-10, Geneva, 1972), p. 161
- 34) For a recent review, see C.B. Dover and J.M. Richard, Annals of Physics 121 (1979) 70.
- 35) R.E. Welsh, *in* Proc. ICOHEPANS 7th, Zurich, 1977 (ed. M.P. Locher) (Birkhäuser Verlag, Basel and Stuttgart, 1977), p. 95.
- 36) M. Izycki et al., *in* Proc. 4th European Antiproton Symposium, Barr-Strasbourg, 1978 (ed. A. Friedman) (Editions du CNRS, Paris, 1979), Vol. 1, p. 3.
- 37) For a review of detection possibilities for X-rays that insist on the energy resolution, see U. Gastaldi, *in* Proc. 4th European Antiproton Symposium, Barr-Strasbourg, 1978 (ed. A. Friedman) (Editions du CNRS, Paris, 1979), Vol. 2, p. 607.
- 38) U. Gastaldi et al., Nuclear Instrum. Methods 156 (1978) 257.
- 39) U. Gastaldi, Nuclear Instrum. Methods, 157 (1978) 441.
- 40) U. Gastaldi, R. Gegenwart, H. Kalinowsky, E. Klempt and O. Schreiber, Detection of 500 eV X-rays with the X-ray drift chamber (XDC) technique, in preparation.

- 41) J. Jeanjean et al., Nuclear Instrum. Methods 117 (1974) 349.
- 42) A. Cordier et al., Nuclear Instrum. Methods 133 (1976) 237.
- 43) Č. Zupančič, π^0 Jacobian peak spectroscopy, CERN \bar{p} LEAR-Note **24** (1979).



- XDC X-ray Drift Chamber
- IDC Internal Drift Chamber
- CMWPC Cylindrical Multiwire Chambers with bidimensional read-out
- PSGD Position Sensitive Gamma Detector
- GD Gamma Detector

Fig. 1

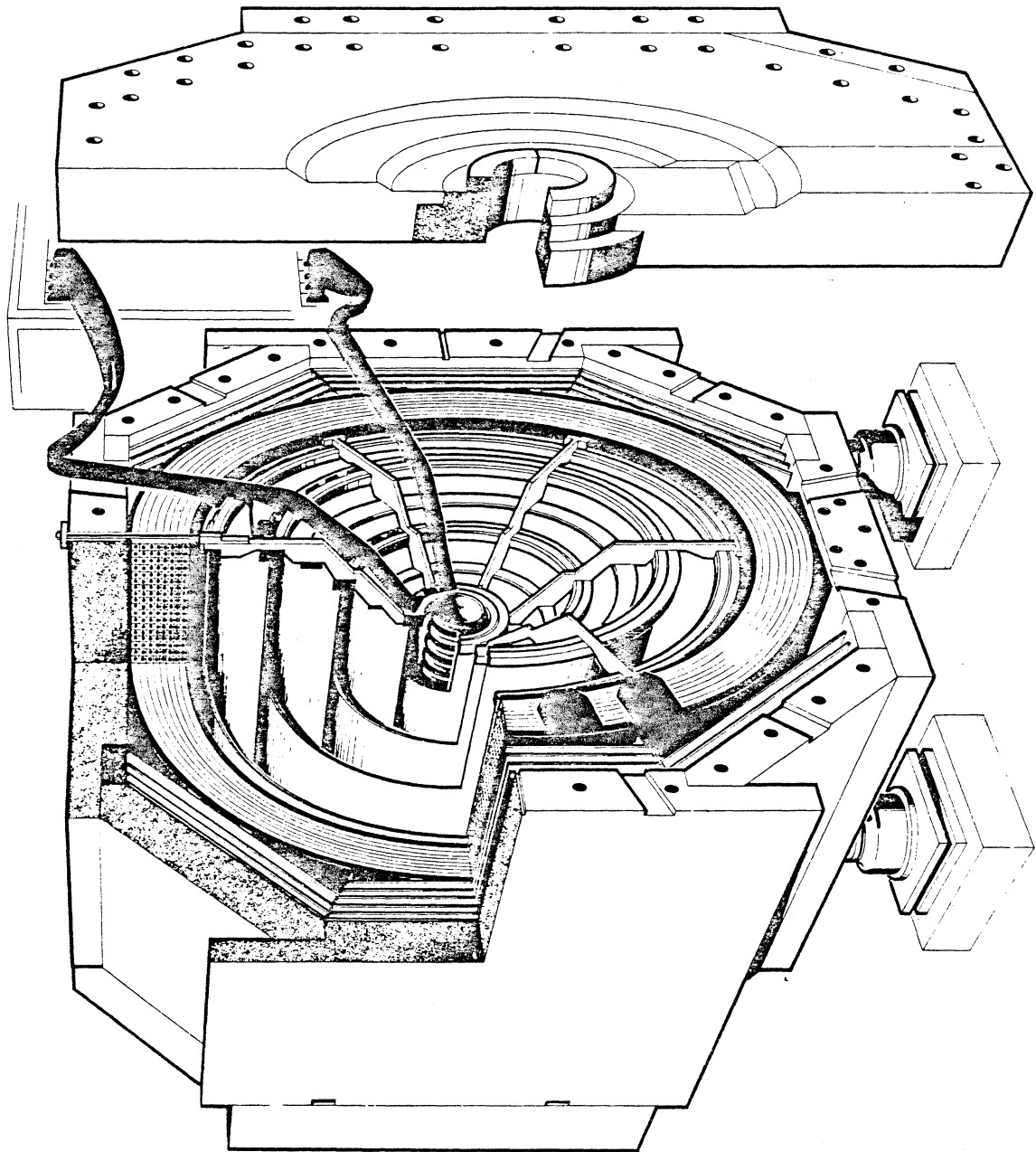


Fig. 2